Smart Structures and Systems, *Vol. 21, No. 5 (2018) 571-582*
DOI: https://doi.org/10.12989/sss.2018.21.5.571

Influence of track irregularities in high-speed Maglev transportation systems

Jing Yu Huang*[1,2], Zhe Wei Wu[1], Jin Shi[3], Yang Gao[4] and Dong-Zhou Wang[1]

[1]*Department of Civil Engineering, Tongji University, Shanghai, China*
[2]*National Maglev Transportation Engineering R&D Center, Tongji University ,Shanghai, China*
[3]*Department of Civil Engineering, Beijing Jiaotong University, Beijing, China*
[4]*Department of Transportation Engineering, Tongji University, Shanghai, China*

(Received December 11, 2017, Revised March 20. 2018, Accepted March 29, 2018)

Abstract. Track irregularities of high-speed Maglev lines have significant influence on ride comfort. Their adjustment is of key importance in the daily maintenance of these lines. In this study, an adjustment method is proposed and track irregularities analysis is performed. This study considers two modules: an inspection module and a vehicle-guideway coupling vibration analysis module. In the inspection module, an inertial reference method is employed for field-measurements of the Shanghai high-speed Maglev demonstration line. Then, a partial filtering, integration method, resampling method, and designed elliptic filter are employed to analyze the detection data, which reveals the required track irregularities. In the analysis module, a vehicle-guideway interaction model and an electromagnetic interaction model were developed. The influence of the measured line irregularities is considered for the calculations of the electromagnetic force. Numerical integration method was employed for the calculations. Based on the actual field detection results and analysis using the numerical model, a threshold analysis method is developed. Several irregularities modalities with different girder end's deviations were considered in the simulations. The inspection results indicated that long-wavelength irregularities with larger girder end's deviations were the dominant irregularities. In addition, the threshold analysis of the girder end's deviation shows that irregularities that have a deviation amplitude larger than 6 mm and certain modalities (e.g., M- and N-shape) are unfavorable. These types of irregularities should be adjusted during the daily maintenance.

Keywords: high-speed Maglev; track irregularities; girder end's deviation; vehicle/guideway coupled model; dynamic response

1. Introduction

Maglev transportation systems are advantageous over the conventional rail-wheel systems in terms of ride quality, running safety, noise reduction, and cost efficiency (Chandra and Agarwal 2013). Therefore, it is more and more important to study Maglev systems with their development in Europe, Japan, Korea, and China over the past two decades. At present, elevated bridges are employed in most Maglev lines. Studies and engineering practices have shown that the Maglev vehicle-guideway coupled vibration is widely present in Maglev systems and poses significant issues, which should be focused on (Zhou *et al.* 2010). Otherwise, using field monitoring data to assess the reliability and stability of elevated bridges is helpful and necessary (Ni *et al.* 2010, Ni *et al*. 2012), which is also important in the estimation and maintenance of maglev line. In general, there are three main types of vibrations that pose issues: moving vehicle-bridge coupled vibration, stationary vehicle-guideway self-excited vibration, and vehicle-guideway interaction vibration in the presence of track irregularities (Zhou *et al.* 2010). In this study, we mainly focus on the third type of vibration of high-speed Maglev vehicles. This vibration amplifies with the increase of the running velocity, and in addition, the irregularities have great impact on the levitation stability (Zhai and Zhao 2005, Yu *et al.* 2015, Zhou *et al*. 2017). Long-wavelength irregularities adjustment is of key importance in the maintenance of high-speed Maglev lines. Therefore, adjustment methods have to be extensively studied and further advanced.

For the adjustment method, track irregularities should be measured and their influence should be estimated. Over the past two decades, extensive studies have been performed on Maglev track irregularities; however, most of them considered random irregularities for the calculations or focused only on middle-low-speed Maglev vehicles. Tsunashima and Abe (1998) proposed the concept of power spectrum density (PSD) of Maglev line's track irregularities. Zhai and Zhao (2005) and Shi e*t al.* (2007) proposed a high-speed Maglev vehicle-guideway interaction dynamic analytical model to compute dynamic responses of girders. They studied the dynamic response for a random-irregularity PSD excitation. Jiang *et al.* (2007) analyzed the dynamic responses of a low-speed maglev vehicle for a sinusoidal excitation. They revealed the influence of track irregularities with different frequencies on vehicle's vertical vibration and proposed levitation control approaches. Zhou *et al.* (2008) calculated vehicle's vertical response PSD using an analytical method of virtual excitation based on the TR08 Maglev vehicle prototype. The proposed method was designed to conveniently and rapidly evaluate riding quality of Maglev vehicles. Jun-Seok *et al.* (2009) developed a numerical model which considers guideway properties and irregularities

*Corresponding author, Professor
E-mail: huangjingyu@tongji.edu.cn

ISSN: 1738-1584 (Print), 1738-1991 (Online)

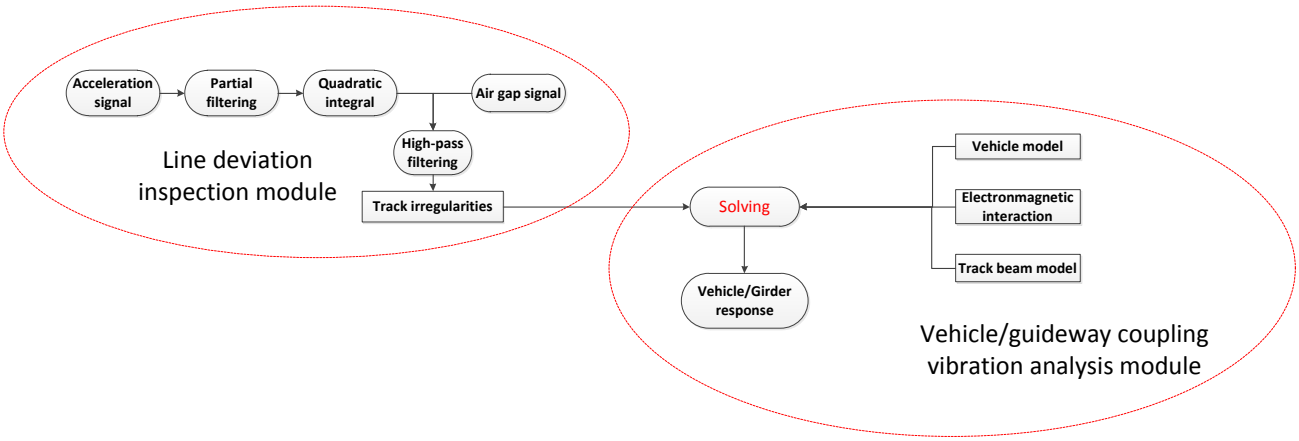

Fig. 1 Framework of the study

to investigate dynamic responses of low and medium speed Maglev systems. Lee *et al.* (2009) considered actual track irregularities of an urban transit Maglev line in Korea in order to study dynamic responses of vehicles and guideways. Min *et al.* (2012) explore the dynamic response under irregularity by considering the nonlinear forms of electromagnetic force and current. Zhou *et al.* (2012) performed a simple stationary test to calculate the PSD function of the track irregularities of the Tangshan low-speed Maglev line in China. Shi *et al.* (2014) employed an inertial reference method to perform a field-test of the Shanghai high-speed Maglev line. They obtained the PSD of the track irregularities; however, its influence was not studied. Talukdar *et al.* (2016) employed the block diagram approach (MATLAB SIMULINK) to examine the effects of vehicle speed and guideway's random-irregularities PSD for the optimization of suspension parameters. Ju *et al.* (2015) investigated the influence of track irregularities caused by foundation settlement, and proposed a proportional-integral (PI) controller to achieve better control. Yu *et al.* (2015) and Zhou *et al.* (2017) studied a low-speed Maglev vehicle levitation module. They studied the random track irregularities in order to reveal the PSD responses of the levitation module, and proposed an adaptive vibration control method to reduce vibrations.

Therefore, extensive studies have been already performed on analysis and management of track irregularities. However, all of them considered hypothetical irregularities in rail-wheel systems for the calculations of dynamic responses of vehicles and guideways. However, the guideway structure of high-speed Maglev lines is very different from that of rail-wheel systems, and in addition, their track irregularities differ (Shi *et al.* 2014). Therefore, suitable models of track irregularities have to be employed in the calculations of vibrations in high-speed Maglev systems. Until now, only several studies on high-speed Maglev lines have been reported, while the track irregularities management methods mainly focused on levitation controllers; adjustment methods of irregularities and their dynamics have not been yet extensively investigated.

This study is a follow-up of a previous study of Shi *et al.* (2014), where an inertial reference method was proposed to investigate characteristics of track irregularities in high-speed Maglev lines. In this study, through track irregularities inspection and analysis of dynamic responses of vehicles and guideways, a track irregularities adjustment method for high-speed Maglev lines is proposed. As shown in Fig. 1, two modules are considered in this study: long-wavelength track-irregularities inspection module and vehicle-guideway coupling vibration analysis module. In the inspection module, the inertial reference method (Shi *et al.* 2014) is employed for a field-test of the Shanghai high-speed Maglev demonstration line in the location range of 19.1 km to 19.45 km, performed in April 2016. The length of the demonstration line is 30 km, the highest operation speed is 431 km/h, while the peak experimental speed is 500 km/h. Then, a series of data processing methods are described to reveal the irregularities. In the analysis module, a 32-degrees-of-freedom (DOFs) vehicle-guideway interaction numerical model is developed to investigate dynamic characteristics of vehicles and guideways with irregularities. The obtained irregularities are employed as the excitation in the calculations. Furthermore, using the results of the actual sample, virtual irregularities are constructed with different end deviations of the girder, which are also employed for the simulations and comparison. The results show that the girder end's deviation adjustment values and adverse track irregularities conditions can be determined, which could be employed in the daily maintenance of high-speed Maglev lines.

2. Track irregularities inspection module

2.1 Processing method

Using the inertial reference method (Shi *et al.* 2014), the relative position h of the guideway contour in an inertial coordinate system can be obtained, as illustrated in Fig. 2. The acceleration a of the magnet is measured by acceleration sensors, which can be used to obtain the relative vertical displacement z of the magnet. The value s is the distance between the magnet of suspension vehicle and stator surface of guideway, namely 'air gap' in maglev transportation, which can be measured by on-board gap sensors. Using Eq. (1), the position h of the guideway contour can be obtained

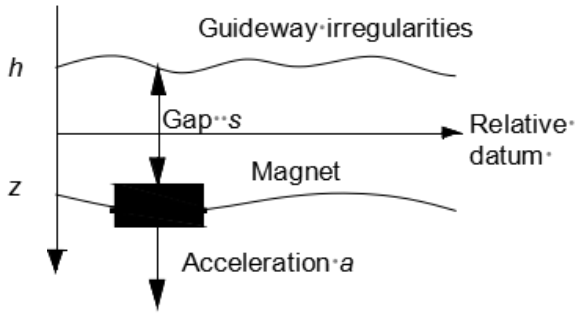

Fig. 2 Irregularities inspection method for high-speed Maglev lines

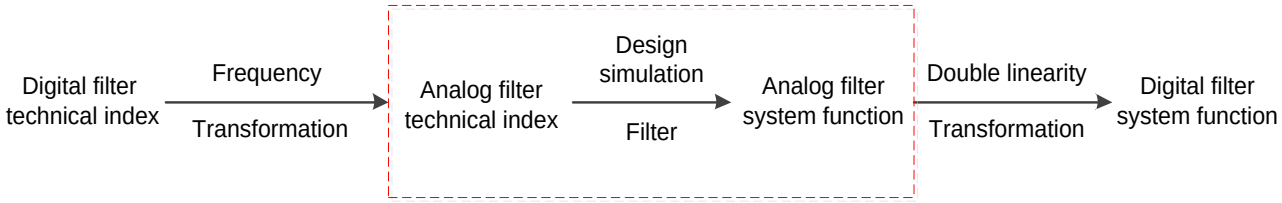

Fig. 3 Filter design flow

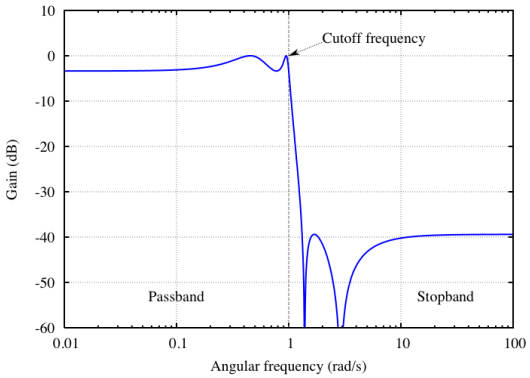

Fig. 4 Frequency response of a fourth-order low-pass elliptic filter

$$h = z - s = \iint a dt^2 - s + c_1 t + c_2 \tag{1}$$

Where c_1 and c_2 are constants that emerge from the integration of the acceleration.

The vertical displacement Z_B of the magnet is obtained by integrating its vibration acceleration $\ddot{Z}_B$

$$Z_B(t) = \iint \ddot{Z}_B(t) dt^2 + C_2 t + C_1 \tag{2}$$

where C_1 and C_2 are constants determined by the initial conditions, which are not important for this analysis. Their existence will eventually lead to a saturation of the integrator. In order to remove their influence, a partial filter (Eq. (3)) is employed (Du *et al.* 1997)

$$R(z) = \frac{(1-\omega_d)(1-z^{-1})}{1-(1-\omega_d)z^{-1}} \tag{3}$$

where ω_d is the cut-off frequency, which determines the damping feature of the filter and transition bandwidth. By employing trial-and-error method, we set the value of ω_d to 1/20000 rad/s.

In order to obtain the displacement value of the electromagnet, the acceleration of the electromagnet should be integrated twice. Taking into account the characteristics of the line inspection system, the rectangular numerical integration method is employed in this study.

The measured track irregularities change with the vehicle running velocity. Therefore, a resampling method is utilized to transform the time signal into a spatial signal, in

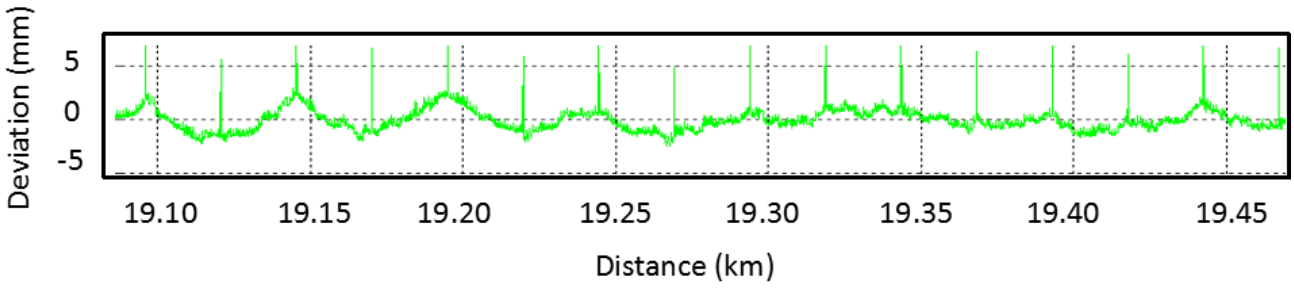

(a) Track irregularities processing results of right side obtained in this study

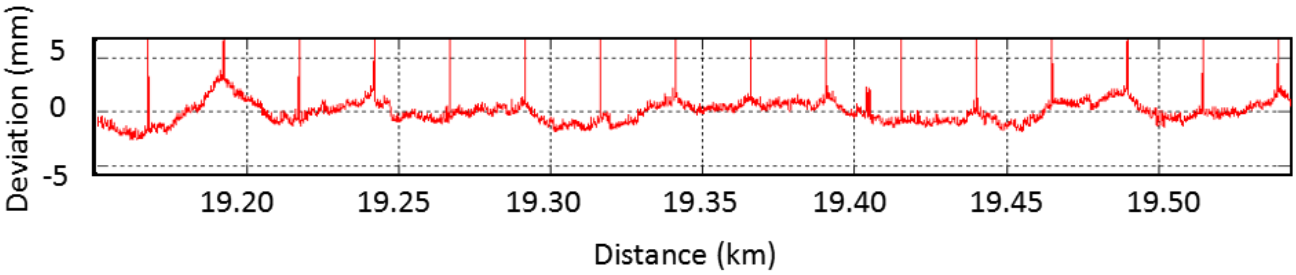

(b) Track irregularities processing results of lef side obtained in this study

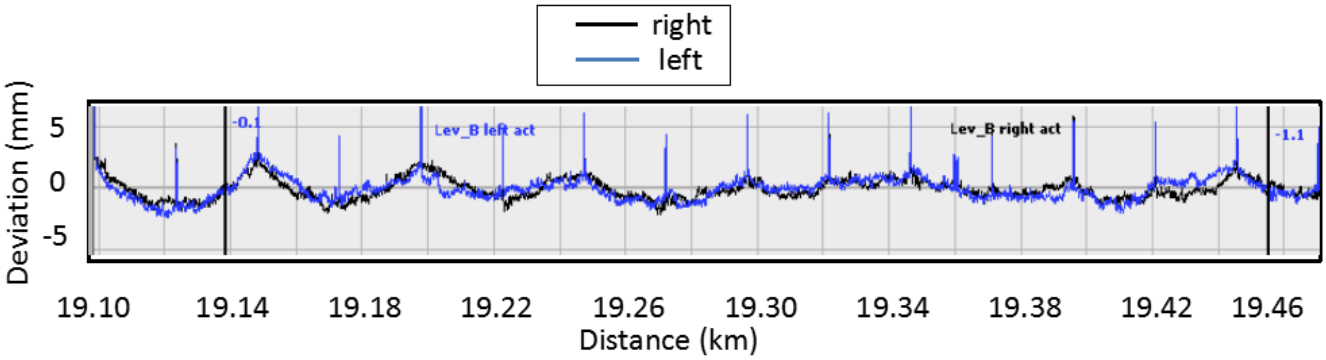

(c) Processing results obtained by German technology supporter of the Shanghai high-speed Maglev line

Fig. 5 Comparison of track irregularities processing results

order to eliminate the influence of the velocity. The space-sampling interval of 86 mm is employed as the sampling pulse to convert the time signal into a spatial signal (Shi *et al*. 2014). After the above procedures, the values of the initial track irregularities are determined. Then, an elliptic filter is designed to filter out the undesired frequency components or random noise in the spectrum of the decaying signal. The design flow of the filter is shown in Fig. 3. The design method is based on the digital filter technical index, and it converts time domain into frequency domain.

The elliptic filter provides equiripple of the stop- and pass-bands, and in addition, it provides minimum fluctuations in the pass- and stop-bands, of the same order; these features are different from those obtained using Butterworth and Chebyshev filters. The amplitude of the frequency response of a low-pass elliptic filter is

$$\left|H(j\omega)\right|^2 = \frac{1}{1+\varepsilon^2 R_N^2(\omega/\omega_c)} \tag{4}$$

where ε is the attenuation of the pass-band, R_N is the n[th]-order Jacobi elliptic function, and ω_c is the cut-off frequency. The frequency response of a fourth-order low-pass elliptic filter is shown in Fig. 4, where the pass-band boundary frequency, stop-band boundary frequency f_s, pass-band attenuation R_p, and stop-band attenuation R_s were set to 1/199 Hz, 1/318 Hz, 4 dB, and 35 dB, respectively.

2.2 Track irregularities processing

In April 2016, a field-test of long-wavelength track irregularities was performed in the location range of 19.1 km to 19.45 km of the Shanghai high-speed Maglev demonstration line. Figs. 5(a) and 5(b) shows the irregularities of the right and left side of the guideway, obtained by using the track irregularities inspection method respectively. Track irregularities which have a wavelength of ~ 50 m can be clearly observed, and the impulses in the peaks and troughs of the waveform are induced by the the

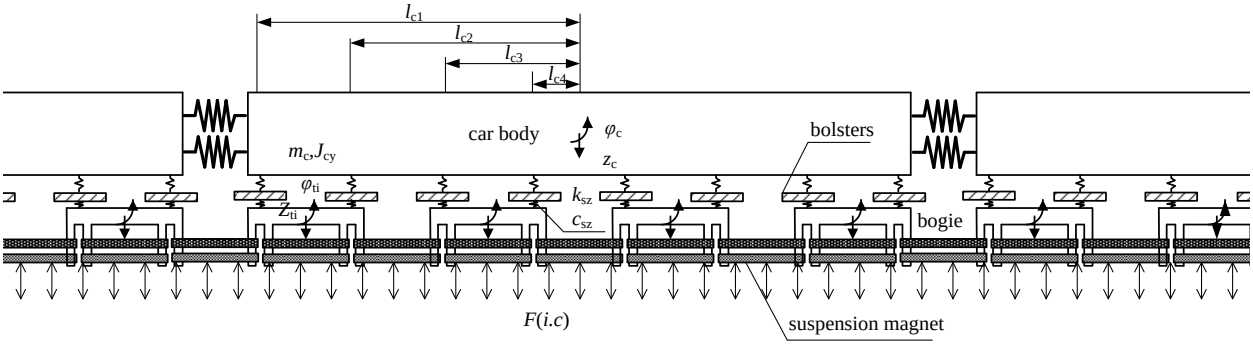

Fig. 6 Vehicle model

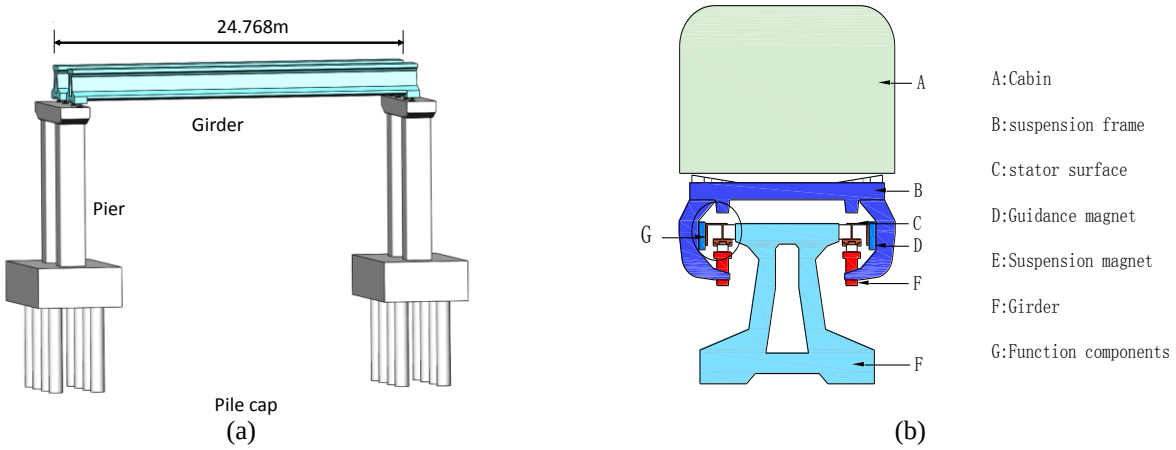

Fig. 7 Illustration of the vehicle and guideway structures

gap between the stators of linear motor which is 90~100 mm at the adjacent girder, and the span length of girder is 24.768 m (Wu and Huang 2004), as shown in Fig. 7. Form the pictures and analysis, it can be concluded that the Maglev line exhibits larger deviations at the end of the girder, long-wavelength track irregularities caused by the girder end's deviation dominate. These processing results can be verified by comparison with those shown in Fig. 5(c), measured by German, which is the engineering technology supporter of the Shanghai high-speed Maglev line.

3. Vehicle-guideway coupling vibration analysis module

3.1 Vehicle-guideway interaction model

The proposed high-speed Maglev vehicle-guideway interaction model consists of a vehicle model and a guideway model. The vehicles comprise several components: cabin, 8 pairs of swinging bolsters, 4 pairs of suspension frames with magnets, and spring-damping suspension devices, as illustrated in Fig. 6.

The vehicle model is simplified to a two-dimensional (2D) numerical model, which has 32 DOFs. They are the cabin vertical motion Z_c (1 DOF), cabin pitch motion α_c (1 DOF), swinging bolsters' vertical motions Z_b (8 DOFs), suspension frame vertical motions Z_t (4 DOFs), suspension frame pitch motions α_t (4 DOFs), electromagnet vertical motions Z_m (7 DOFs), and electromagnet pitch motions α_m (7 DOFs).

The guideway structure consists of girders, piers, and functional components, as shown in Figs. 7(a) and 7(b).

In order to decrease the number of computational DOFs, the modal superposition method is introduced in the guideway model. First, the vibration frequencies and modes of vibration of the guideway are calculated. Then, using the orthogonality of the vibration modes, the equations of the nodes, coupled with each other, are decoupled so that they can be transformed into independent modal equations (Xia and Guo 2008). It is reasonable to suppose that there is no relative displacement between the guideway girder and functional components. Therefore, the vibration mode of a pier node is identical to that of the corresponding girder node. The mode of vibration between two nodes is determined by the Lagrange interpolation method; the cross-section deformation is neglected in the vibration analysis. Using the expansion theorem, the nth girder modal equation can be expressed as

Table 1 Parameters of the high-speed Maglev system

Symbol	Quantity	Value
m	Total weight of suspended object	700 kg
A	Pole face area	356 cm^2
N	Number of turns in the magnet winding	300
μ_0	Air permeability	4×10^{-7} H/m
$c(t)$	Magnetic air gap	0.01 m
k_p	Feedback gain that corresponds to the air gap change	6000
k_v	Feedback gain that corresponds to the velocity of the magnet	60
k_a	Feedback gain that corresponds to the acceleration of the magnet	1

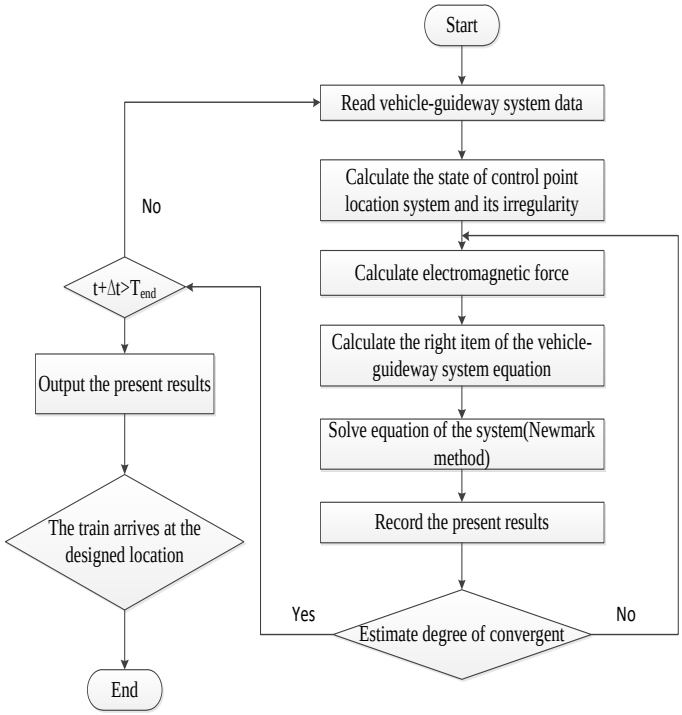

Fig. 8 Flow diagram of the developed program

$$\ddot{q}_n + 2\xi_n\omega_n\dot{q}_n + {\omega_n}^2 q_n = F_n \tag{5}$$

where ξ_n and ω_n are the damping ratio and natural frequency of the nth vibration mode, respectively, while F_n is the generalized force, which is the product of the magnetic force and vibration mode $\psi(x)$.

The displacement Z_{kdz} of the girder can be expressed as

$$Z_{kdz} = \sum_{n=1}^{N_b} q_n \varphi_v^n(x) \tag{6}$$

where q_n is the generalized coordinate, $\phi_v^n(x)$ is the vertical vector of the nth mode, N_b is the number of modes.

The displacement Z_{kdijk} of the k^{th} control point of the j^{th} suspension frame of the i^{th} vehicle on the girder can be expressed as the superposition of the girder displacement and track irregularities Z_s

$$Z_{kdijk} = \sum_{n=1}^{N_b} q_n \varphi_v^n(x_{ijk}) + Z_s(x_{ijk}) \tag{7}$$

By combining the vehicle model and guideway girder model, the vehicle-guideway interaction dynamic equation can be expressed as

$$\begin{bmatrix} \mathbf{M}_{vv} & \mathbf{0} \\ \mathbf{0} & \mathbf{M}_{bb} \end{bmatrix} \begin{Bmatrix} \ddot{\mathbf{X}}_v \\ \ddot{\mathbf{X}}_b \end{Bmatrix} + \begin{bmatrix} \mathbf{C}_{vv} & \mathbf{C}_{vb} \\ \mathbf{C}_{bv} & \mathbf{C}_{bb} \end{bmatrix} \begin{Bmatrix} \dot{\mathbf{X}}_v \\ \dot{\mathbf{X}}_b \end{Bmatrix} + \begin{bmatrix} \mathbf{K}_{vv} & \mathbf{K}_{vb} \\ \mathbf{K}_{bv} & \mathbf{K}_{bb} \end{bmatrix} \begin{Bmatrix} \mathbf{X}_v \\ \mathbf{X}_b \end{Bmatrix} = \begin{bmatrix} \mathbf{F}_{vb} \\ \mathbf{F}_{bv} \end{bmatrix} \tag{8}$$

Where $\boldsymbol{M}$,$\boldsymbol{K}$,$\boldsymbol{C}$ are the mass, stiffness, and damping matrices of the vehicle-guideway system, respectively, $\boldsymbol{X}, \dot{\boldsymbol{X}}, \ddot{\boldsymbol{X}}$ are the displacement, velocity, and acceleration vectors, respectively, $\boldsymbol{F_{vb}}, \boldsymbol{F_{bv}}$ are the interaction forces

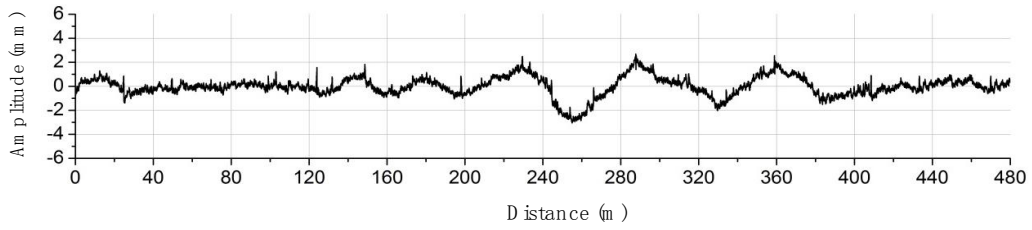

Fig. 9 Track irregularities of the guideway, obtained by performing a field-test

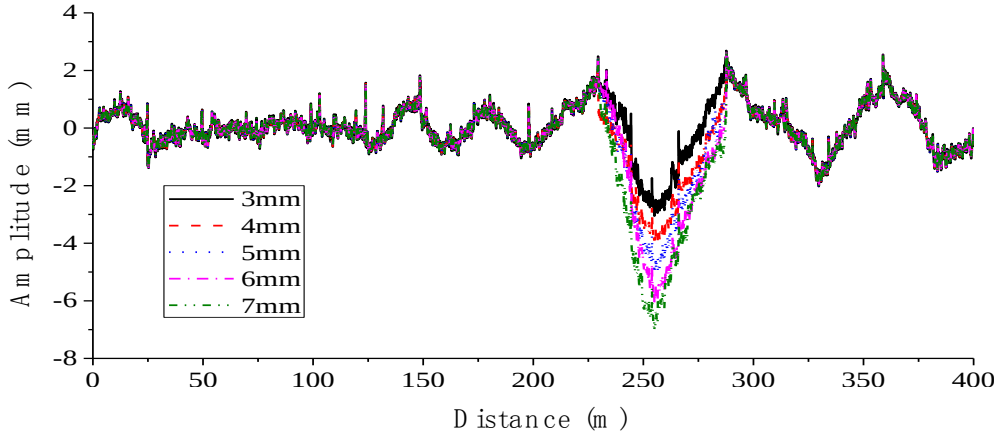

Fig. 10 Virtual track irregularities for different end-deviations of the girder

between the vehicle and guideway, and the subscripts v and b correspond to the vehicle and guideway, respectively.

3.2 Electromagnetic guideway interaction force

The decoupling concept of multiple-points independent-suspension-guidance control systems is employed for the Maglev vehicle, which provides the vehicle with mechanical flexibility and mechanical statically. Single-point suspension system is the basic unit of the electromagnetic action. Using the electromagnetic theory proposed by Sinha (1987), the electromagnet attractive force F as a function of the time is

$$F(i,c) = \frac{u_0 N^2 A}{4}\left[\frac{i(t)}{c(t)}\right]^2 \tag{9}$$

where N is the number of turns of the coil, u_0 is the magnetic permeability of the vacuum, A is the effective area of the magnetic pole, $i(t)$ is the current in the circuit, and $c(t)$ is the air gap between the magnet and stator surface of the guideway.

As the open-loop system has an inherent instability, the air gap variation has to be controlled within a predefined error range using the closed-loop feedback control method. There are many developed programs which can be employed for a current feedback control. For the high-speed Maglev systems, feedback programs for the position, velocity, and acceleration of the air gap variations, can be employed (Shi *et al*. 2007)

$$\Delta i(t) = k_p \Delta c(t) + k_v \Delta \dot{z}(t) + k_a \Delta \ddot{z}(t) \tag{10}$$

where k_p, k_v, and k_a are the position, velocity, and acceleration feedback coefficients, respectively, $\Delta c(t)$ is the air gap change, $\Delta z(t)$ represents the change of the displacement of the suspended. The employed parameters are listed in Table 1 (Shi *et al.* 2007).

Based on the above analysis, a computer program was developed to perform dynamic analysis; its flow diagram is illustrated in Fig. 8.

4. Threshold analysis for the control of track irregularities

In the current practice for the maintenance of the Shanghai high-speed Maglev line, the end deviation of the girder is adjusted to manage the irregularities. Accordingly, it is necessary to investigate the effects of the girder end's deviation on the dynamic responses of the vehicle and guideway. In this study, using the field-measured track irregularities, several types of track irregularities with different amplitude scales are simulated, which is utilized to perform comparative studies.

Using the field-measured track irregularities (Fig. 9), virtual track irregularities are constructed by setting the amplitude of the girder end's deviation to 3, 4, 5, 6, and 7 mm at a distance of 250 m from the measured line, as

Table 2 Vehicle operation indices as a function of the girder end's deviation

Deviation (mm)	Largest acceleration of the vehicle (m/s^2)	Largest gap variation (mm)	Largest acceleration of the beam's mid-span (m/s^2)
3	0.16	1.5	1.25
4	0.25	1.5	2.25
5	0.27	1.5	2.43
6	0.32	2.1	2.48
7	0.32	2.7	2.5

shown in Fig.10. The running velocity is set to 431 km/h, in order to consider the unfavorable conditions.

Track irregularities with five different amplitudes are considered for the excitation in the simulations to examine the effect of the amplitude of the girder end's deviation.

By performing simulations using the numerical vehicle-guideway model, the dynamic characteristics of the vehicle and guideway are obtained. The calculated variations of the vertical acceleration, variations of the air gap, deformation of the girder, and acceleration of the girder mid-span, are presented in Figs as follows. Fig. 11 shows the comparision of the vehicle's vertical vibration accelerations under different girder-end deviations, and the Figs. 13(a)-13(e) are their acceleration respectively. Figs.11 and 13 suggests that the end-deviation of the girder leads to an obvious vertical vibration of the cabin. Fig.12 shows that the suspension air gap varies under different girder-end deviations, and Figs. 14(a)-14(e) are their variations respectively. Figs.16 and 18 show that the vibration of the girder increases with the deviation amplitude; however, from the Figs. 15 and 17, it can be found that the deviation has only a small influence on the vertical deformation of the girder

Furthermore, by analyzing the peak value of the cabin vibration, suspension gap variations, and girder acceleration, the relationships between the girder end's deviation and cabin vertical acceleration, suspension gap variations, and mid-span acceleration of the girder, can be obtained, as shown in Fig. 19 and Table 2. The largest vehicle acceleration increases with the girder end's deviation. It rapidly increases in the deviation range of 0 mm to 4 mm, while for deviations larger than 6 mm the increase is slower. However, it is worth noting that the largest vehicle acceleration never exceeds the value of 0.4 m/s^2. According to the passengers' comfort standard, China's national standard GB5599-85, the allowable value of the largest vertical acceleration is set to 0.4 m/s^2.

Therefore, the vertical acceleration should comply with the requirements. Fig. 19 shows that the largest gap variation increases slowly when the deviation is in the range of ~ 0 mm to ~ 3 mm; it rapidly increases for deviations larger than 3 mm. Table 2 shows that for a deviation of 6 mm, the gap variation can reach a value of 2.1 mm, which exceeds the 2-mm-range of the deviation adjustment. Moreover, Fig. 20 shows that the largest acceleration of the girder mid-span increases rapidly for deviation values in the range of 0 mm to 4 mm; the increase of the largest acceleration is slower for deviations larger than 4 mm. The acceleration can reach a value of 2.5 m/s^2, when the deviation is 6 mm.

The above analysis shows that when the deviation is larger than 6 mm, the gap variation exceeds the adjustment range of 2 mm. In addition, the simulation result in Fig.21 shows that when the deviation is larger than 8 mm, for a running velocity of 500 km/h, a collision will occur between the suspension magnet and guideway, which certainly has to be avoided in high-speed Maglev lines. Therefore, the girder end's deviation should be controlled below 6 mm.

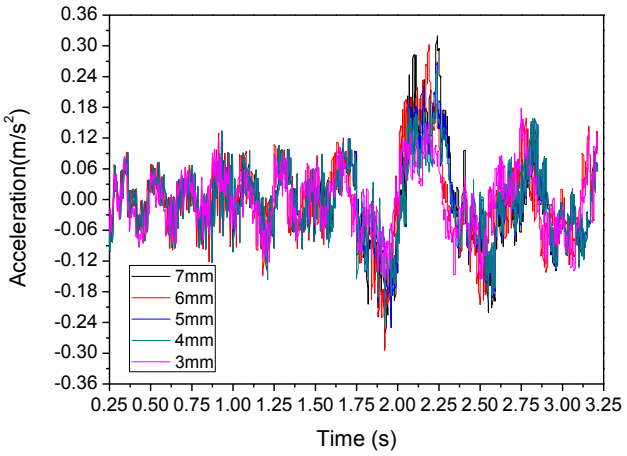

Fig. 11 Time-history of the vehicle's vertical acceleration

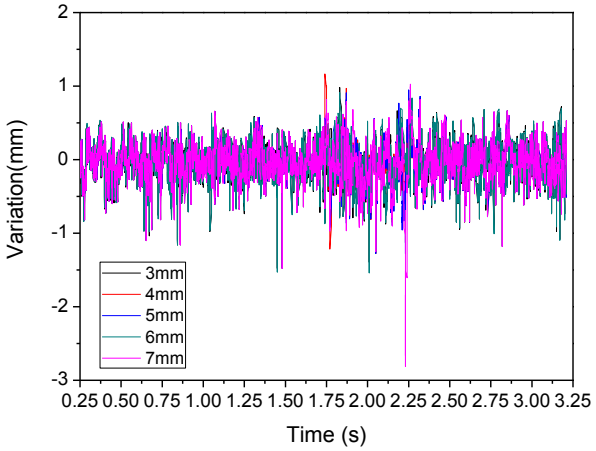

Fig. 12 Time-history of the air gap variations

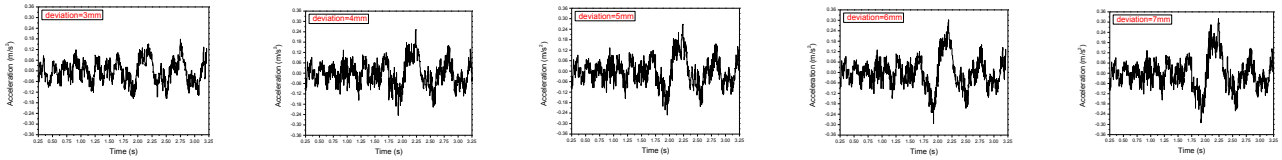

(a) 3 mm (b) 4 mm (c) 5 mm (d) 6 mm (e) 7 mm

Fig. 13 Time-history of the vehicle's vertical acceleration

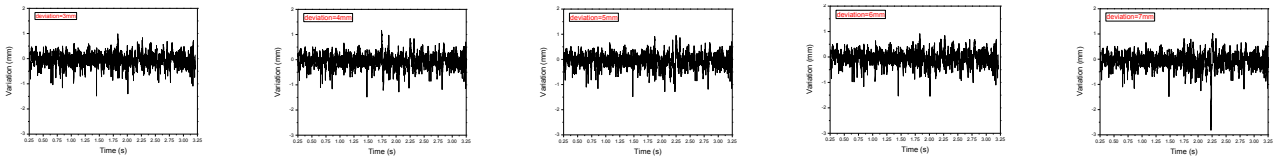

(a) 3 mm (b) 4 mm (c) 5 mm (d) 6 mm (e) 7 mm

Fig. 14 Time-history of the vehicle's vertical acceleration

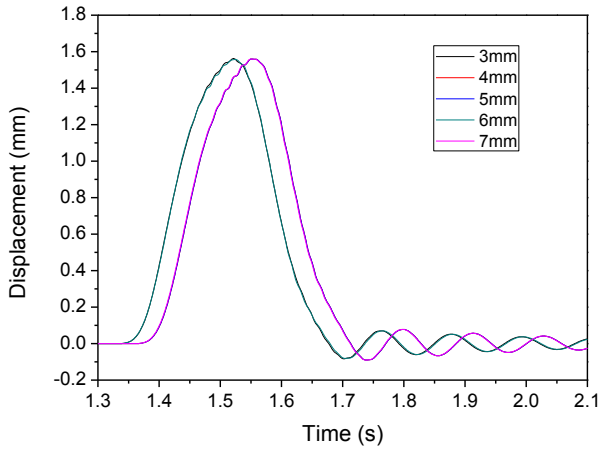

Fig. 15 Dependence of time history of mid-span displacement of girder under different deviations

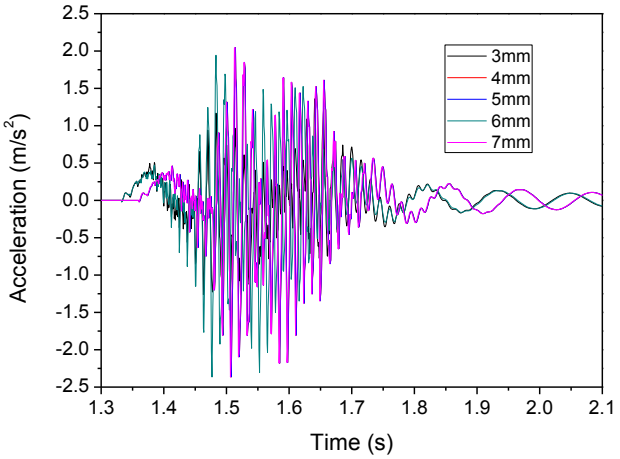

Fig. 16 Dependence of time history of mid-span acceleration of girder. Under different deviations

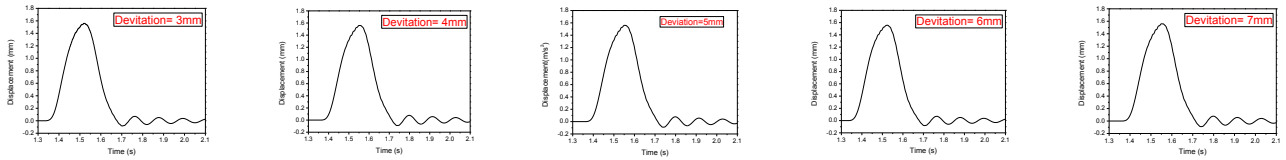

(a) 3 mm (b) 4 mm (c) 5 mm (d) 6 mm (e) 7 mm

Fig. 17 Time history of mid-span displacement of girder

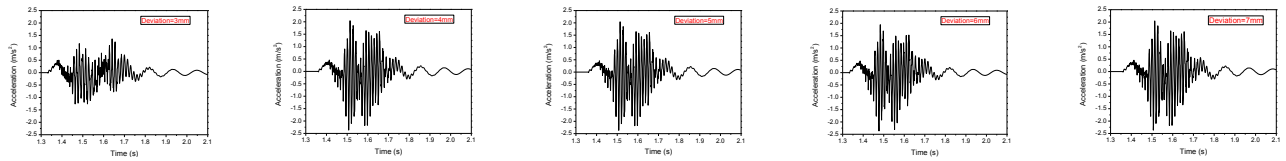

(a) 3 mm (b) 4 mm (c) 5 mm (d) 6 mm (e) 7 mm

Fig. 18 Time history of mid-span acceleration of girder

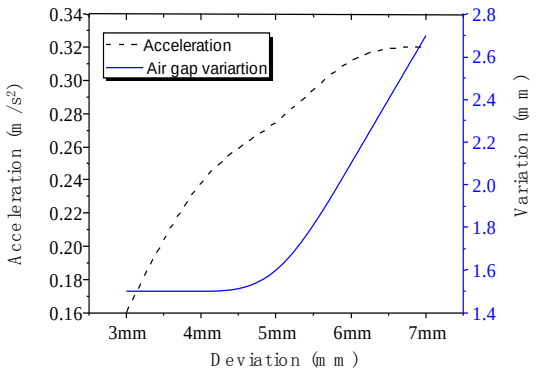

Fig. 19 Dependences of the largest acceleration of the vehicle and gap variation as a function of the girder end's deviation

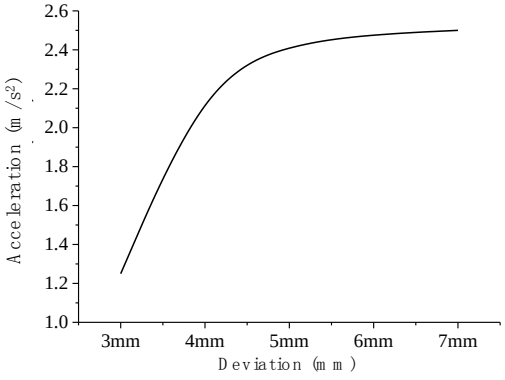

Fig. 20 Dependence of the largest acceleration of the girder's mid-span as a function of the end deviation

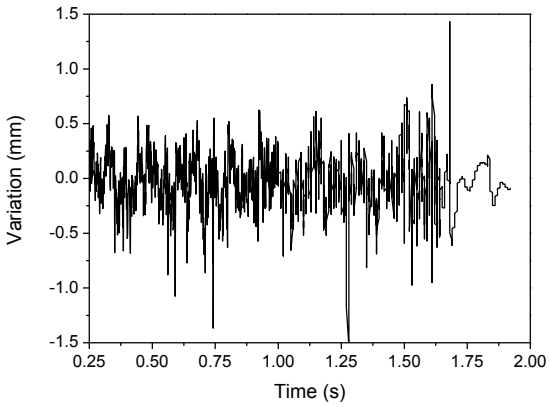

Fig. 21 Time-history of the air gap variations for a running velocity of 500 km/h

4.1 Calculations for different shapes of track

Based on the field-measured track irregularities, V-, M-, and N-shape irregularities investigate the effects of the shape of the irregularities, as shown in Fig. 19. For the simulations, the amplitude was set to 7 mm, the span length of the girder was set to 24.768 m, and the running velocity was set to 431 km/h.

4.2 Analysis of the results

Fig. 20 shows the dynamic responses for three different shapes of track irregularities. It can be noticed that the largest accelerations of the vehicle are 0.23 m/s^2, 0.38 m/s^2, and 0.38 m/s^2 for the V-, M-, and N-shape deviations, respectively. Fig. 21 indicates the largest gap variations are 1.8 mm, 4.1 mm, and 4.1 mm for the V-, M-, and N-shape deviations, respectively. Therefore, it can be concluded that the M- and N-shape deviations can amplify the vibration of the vehicle, i.e., increase the air gap variations, which is unfavorable.

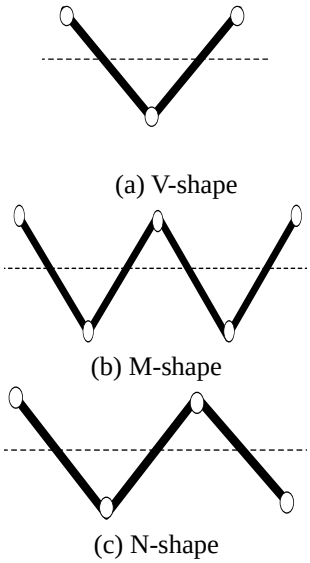

Fig. 22 End deviation's shapes.

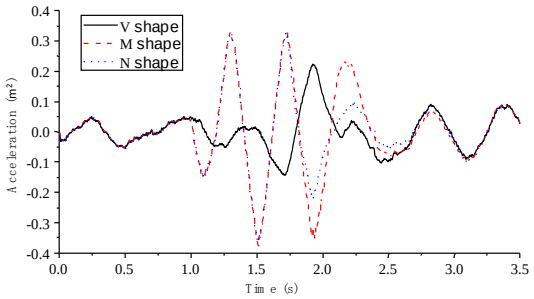

Fig. 23 Vehicle accelerations for different shapes of deviations

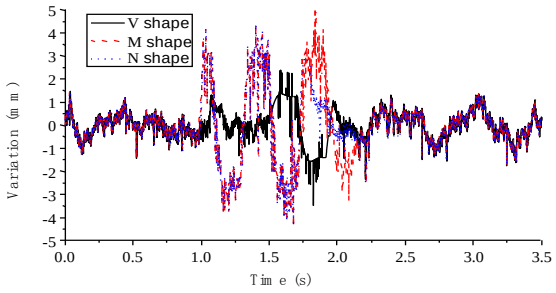

Fig. 24 Air gap variations for different shapes of deviations

5. Conclusions

Track irregularities of high-speed Maglev lines were studied. A vehicle-guideway dynamic interaction model was developed to study the dynamic responses of vehicles and guideways. Girder end's deviation threshold analysis method was developed. Using the results of the threshold analysis, several conclusions can be summarized, as follows.

- An inertial reference method is applied to detect the track irregularities, and the detection data is processed by a partial filtering, integration method, resampling method, and designed elliptic filter. After that, the results are obtained, which are similar to those obtained by German's technology team, both performed at the same field-measurement position of the Shanghai high-speed Maglev line. This shows that the inertial reference and data processing methods are effective for characterization of irregularities in high-speed Maglev lines.
- The samples that have long-wavelength track irregularities show larger girder end's deviations. This implies that it is necessary to improve the installation accuracy of guideways during construction. In addition, effective approaches should be developed to measure the girder end's deviation and reduce the impact of the irregularities by adjusting the deviation.
- The threshold analysis shows that the girder end's deviation has only a small influence on the vertical deformation of the girder. But the vertical acceleration of the vehicle rapidly increases with the increase of the girder end's deviation (for deviations smaller than 4 mm), and the acceleration can meet the requirements of ride comfort. The increase is slower for deviations larger than 6 mm, and in addition, the air gap variations exceed the variation range of 2 mm. Moreover, the suspension magnet will collide with the stator surface when the deviation exceeds 8 mm, for a running velocity of 500 km/h. Therefore, to ensure ride safety and comfort, girder end's deviation should not exceed 6 mm, which should be considered in the maintenance of high-speed Maglev lines.
- M-shape and N-shape track irregularities could amplify the vehicle vibration, and increase the air gap variations. This should be prevented by employing adjustment methods of track irregularities in high-speed Maglev lines.

Acknowledgments

The research described in this paper was financially supported by the National 12th Five-Year Science and technology support program (Project No:2013BAG19B01).

References

Chandra, S. and Agarwal, M.M. (2013), "Maglev trains", *Railway Engineering*, (**October**), 617.

Deng, Y.Q., Luo, S.H., Liang, H.Q., Ma,W.H. (2007), "Simulation model of maglev coupling dynamics performance based on SIMPACK", *J. Traffic Transportation Eng.*, **7**(1), 12-16.

Du, H.T., Gao, L.K. and Fan, Y.P. (1997), "Application of digital filtering technology in track inspection", *Chinese of Railway Scienc*e, **18**(1) (in chinese).

Jiang, H.B., Luo, S.H. and Dong, Z.M. (2007), "Influence of track irregularity to the low-speed maglev vehicle dynamic response", *Railway Locomotive & Car*, **27**(3), 30-32.

Ju, S.H., Leong, C.C. and Ho, Y.S. (2015), "Control of Maglev trains moving on Bridges during foundation settlements", *International Conference on Computer Information Systems*

and Industrial Applications (CISIA 2015)

Lee, J.S., Kwon, S.D., Kim, M.Y. and Yeo, I.H. (2009), "A parametric study on the dynamics of urban transit Maglev vehicle running on flexible guideway bridges", *J. Sound Vib.*, **328**, 301-317

Min, D.J., Lee, J.S. and Kim, M.Y. (2012), "Dynamic interaction analysis of actively controlled maglev vehicles and guideway girders considering nonlinear electromagnetic forces", *Coupled Syst. Mech.*, **1**(1), 39-57

Ni, Y.Q., Ye, X.W. and Ko, J.M. (2010), "Monitoring-based fatigue reliability assessment of steel bridges: analytical model and application", *J. Struct. Eng. - ASCE*, **136**(12), 1563-1573.

Ni, Y.Q., Ye, X.W. and Ko, J.M. (2012), "Modeling of stress spectrum using long-term monitoring data and finite mixture distributions", *J. Eng. Mech. - ASCE*, **138**(2), 175-183.

Shi, J., Fang, W.S., Wang, Y.J. and Zhao, Y. (2014), "Measurements and analysis of track irregularities on high speed maglev lines", *Zhejiang Univ-Sci A(Appl phys&Eng)*, **15**(6), 385-394

Shi, J., Wei, Q.Z. and Zhao, Y. (2007), "Analysis of dynamic response of the high-speed EMS Maglev vehicle/guideway coupling system with random irregularities", *Vehicle Syst. Dyn.*, **45**(2), 1077-1095

Sinha, P.K. (1987), "Electromagnetic suspension dynamic control", *Peter Peregrinus Ltd.*

Talukdar, R.P. and Talukdar, S. (2016), "Dynamic analysis of high-speed Maglev vehicle-Guideway system: an approach in block diagram environment", *Urban Rail Transit*, **2**(2), 71-84

Tsunashima, H. and Abe, M. (1998), "Static and dynamic performance of permanent magnet suspension for Maglev transport vehicle", *Vehicle Syst. Dyn.*, **29**(2), 83-111

Wu, X.M. and Huang, J.Y. (2004), "Guideway Structure, Maglev Demonstration Line, Shanghai", *Structural Engineering International: Journal of the International Association for Bridge and Structural Engineering*, **11**(1).

Xia, H. and Guo. W.W. (2008), "Lateral dynamic interaction analysis of a train-girder-pier system", *J. Sound Vib.*, **31**(8), 927-942.

Yu, P.C., Li, J.H., Li, J. and Wang, L.C. (2015), "Influence of track periodical irregularities to the suspension system of low-speed maglev vehicle", *Proceedings of the 34th Chinese Control Conference*

Zhai, W.M. and Zhao, C.F. (2005), "Dynamics of Maglev vehicle/guideway system (I)-magnet/rail interaction and system stability", *Chinese J. Mech. Eng.*, **41**(7), 1-10. (in chinese)

Zhou, D.F., Yu, P.C., Wang, L.C. and Li, J. (2017), "An adaptive vibration control method to suppress the vibration of the maglev train caused by track irregularities", *J. Sound Vib.*, **408**, 331-350

Zhou, D.F., Hansen, C.H., Li, J. and Chang, W.S. (2010), "Review of coupled vibration problems in EMS Maglev vehicles", *Int. J. Acoust. Vib.*, **15** (1), 10-23

Zhou, J.S., Li, D.G. and Shen, G. (2008), "Pseudo-excitation analysis method of riding quality for maglev vehicle", *J. Traffic Transportation Eng.*, **8**(1), 5-9.